UNIVERSIDADE FEDERAL DO PARÁ
INSTITUTO DE GEOCIÊNCIAS
FACULDADE DE GEOFÍSICA

DANIELA COSTA MELO

1D LATERALLY CONSTRAINED INVERSION OF 2D MT DATA

BELÉM
2017

DANIELA COSTA MELO

1D LATERALLY CONSTRAINED INVERSION OF 2D MT DATA

Undergraduate thesis submitted to Faculty of Geophysics of the Universidade Federal do Pará for obtaining a Bachelor of Science degree in Geophysics.

Supervisor: Prof. Dr. Cícero Roberto Teixeira Régis

BELÉM
2017

Dados Internacionais de Catalogação-na-Publicação (CIP)
Biblioteca do Instituto de Geociências/SIBI/UFPA

Melo, Daniela Costa, 1994 -

1D laterally constrained inversion of 2D MT data / Daniela Costa Melo. – 2017.

34 f. : il. ; 30 cm

Inclui bibliografias

Orientador: Cícero Roberto Teixeira Régis

Trabalho de Conclusão de Curso (Graduação) – Universidade Federal do Pará, Instituto de Geociências, Faculdade de Geofísica, Belém, 2017.

1. Prospecção - Métodos geofísicos. 2. Geofísica. 3. Prospecção magnetotelúrica. I. Título.

CDD 22. ed.: 622.15

DANIELA COSTA MELO

1D LATERALLY CONSTRAINED INVERSION OF 2D MAGNETOTELLURIC DATA

Trabalho de Conclusão de Curso apresentado à Faculdade de Geofísica do Instituto de Geociências da Universidade Federal do Pará, como requisito parcial à obtenção de grau de Bacharel em Geofísica.

Data da defesa: 10 de março de 2017.
Conceito: EXC
Banca Examinadora:

Prof. Cícero Roberto Teixeira Régis - Orientador
Doutor em Geofísica
Universidade Federal do Pará

Prof. Edelson da Cruz Luz - Membro
Doutor em Geofísica
IFPA, Marabá

Prof. Marcos Welby Correa Silva - Membro
Doutor em Geofísica
Universidade Federal do Pará

This work is dedicated to my parents, José Mauricio and Divanir Costa, for always prioritizing my education.

ACKNOWLEDGEMENTS

I thank God for the strength, comfort and security I have received so far.

To all my family and friends, especially my parents José Mauricio and Divanir, who invested in my education and always encouraged me to achieve what I wanted.

To my boyfriend and best friend Andrey Marcos for the fellowship and help during the long hours of study.

To the professors of the Faculty of Geophysics (FAGEOF-UFPA) for the knowledge taught throughout the graduation.

To Capes for the Sandwich Graduation in the United States, throughout The Science Without Borders Program (CsF), which I consider a unique and special experience that I had the opportunity to live.

To the teachers of Colorado School of Mines: Paul Sava, Walt Lynn, John Stockwell, Roel Snieder, Andrei Swidinsky, Thomas Davis and Terry Young for the learning during the two semesters of exchange.

Thanks also to senior researcher Dr. Bob Hardage for giving me an internship opportunity, assisting him in his research.

To my advisor, prof. Dr. Cicero Régis, for all the teaching passed on during his classes and orientation meetings. Moreover, for the incentive and fundamental contribution to the development of this work.

To PETROBRAS for the financing of this research, through project number 0050.0088121.13.9–UFPA/FADESP/PETROBRAS, part of the Research Network of Applied Geophysics.

To all others who, directly or indirectly, contributed to the accomplishment of this work.

ABSTRACT

Applying 1D inversion to 2D magnetotelluric data allows the geophysicist to obtain fast and meaningful results, despite the inherent limitation of trying to approximate the subsurface response by models that vary only in one direction. This paper presents a way to minimize this limitation by performing the inversion of a set of MT soundings with constraints that take into account the lateral variations in the resistivity of the subsurface. The data from all sounding stations in an MT survey line are inverted jointly, producing layered columns with lateral smooth transitions. This process takes advantage of the low computational cost of 1D inversions, and it generates an approximate 2D model that can be useful as a first guess in a full 2D inversion. Two synthetic examples are used to evaluate the practical utility of the algorithm.

Keywords: Data inversion. Regularized inversion. Lateral constraints.

RESUMO

A inversão 1D de dados magnetotelúricos 2D permite ao geofísico obter resultados rápidos e significativos, apesar da limitação inerente de tentar aproximar a resposta da subsuperfície por modelos que variam apenas em uma direção. Este trabalho apresenta uma forma de minimizar esta limitação, realizando a inversão de um conjunto de sondagens MT com restrições que levam em consideração as variações laterais na resistividade da subsuperfície. Os dados de todas as estações de sondagem de uma linha de levantamento MT são invertidos em conjunto, produzindo colunas estratificadas com transições laterais suaves. Esse processo aproveita o baixo custo computacional das inversões 1D e gera um modelo 2D aproximado que pode ser útil como uma primeira suposição em uma inversão 2D completa. Dois exemplos sintéticos são usados para avaliar a utilidade prática do algoritmo.

Palavras-chave: Inversão de dados. Inversão regularizada. Vínculos laterais.

LIST OF FIGURES

Figure 1 Example of the organization of parameters in a 2D structure. The red triangles represent sounding stations. 12

Figure 2 Section view of model 1. 17

Figure 3 TM mode apparent resistivity and phase pseudo sections. 18

Figure 4 Resistivity models obtained by 1D inversion using (a) Global Smoothness and (b) Total Variation regularization in the vertical direction and no lateral constraints. 19

Figure 5 Resistivity models obtained by 1D LCI using (a) GS ($\lambda = 10^4$, $\alpha_V = 5 \times 10^{-7}$ and $\alpha_H = 5 \times 10^{-6}$) and (b) TV ($\lambda = 10^4$, $\alpha_V = 10^{-5}$, $\alpha_H = 10^{-4}$ and $\beta = 10^{-3}$) regularizations in both vertical and lateral directions. 21

Figure 6 Data fitting curves for the 1D LCI using GS: positions (a) $x = -5$km, (b) $x \simeq -0.55$km and (c) $x = 5$km. 23

Figure 7 Data fitting curves for the 1D LCI using TV: positions (a) $x = -5$km, (b) $x \simeq -0.55$km and (c) $x = 5$km. 24

Figure 8 Section view of the model 2. 25

Figure 9 TM mode apparent resistivity and phase pseudo sections. 26

Figure 10 Resistivity models obtained by 1D inversion using (a) GS and (b) TV regularizations in the vertical direction and no lateral constraints. 27

Figure 11 Resistivity models obtained by 1D LCI using (a) GS ($\lambda = 10^4$, $\alpha_V = 10^{-5}$ and $\alpha_H = 3 \times 10^{-4}$) and (b) TV ($\lambda = 10^4$, $\alpha_V = 10^{-4}$, $\alpha_H = 5 \times 10^{-4}$ and $\beta = 10^{-2}$) regularizations in both vertical and lateral directions. 28

Figure 12 Data fitting curves for the 1D LCI using GS: positions (a) $x \simeq -0.57$km above the first block (b) $x = 0$km right in the middle of the two blocks and (c) $x \simeq 0.57$km above the second block. 30

Figure 13 Data fitting curves for the 1D LCI using TV: positions (a) $x \simeq -0.57$km above the first block (b) $x = 0$km right in the middle of the two blocks and (c) $x \simeq 0.57$km above the second block. 31

CONTENTS

1 INTRODUCTION 10

2 METHODOLOGY 11

2.1 **Inversion theoretical revision** 12

2.1.1 Regularized Inverse Problem 13

2.1.1.1 Global Smoothness 13

2.1.1.2 Total Variation 14

2.1.2 Gauss-Newton method with Marquardt's strategy 15

3 APPLICATION 17

3.1 **Model 1** 17

3.2 **Model 2** 25

4 CONCLUSION 33

REFERENCES 34

1 INTRODUCTION

The interpretation of magnetotelluric (MT) data can be done either qualitatively, by means of the apparent resistivity an phase pseudo-sections, or by solving the inverse problem, which consists in determining the geo-electrical structures from the geophysical data. Starting with the observed data and a physical law, it is possible to obtain the parameters of an interpretive model of the subsurface. However, this is a difficult problem because of the complexity of the Earth's interior structures and the lack of enough information in the observed data to resolve those structures.

1D inversion of data from a single sounding station can be performed to resolve the resistivities of a layered interpretive model composed by a number of homogeneous layers over a homogeneous half-space. In this case, the forward modeling problem is a fast and accurate implementation of an analytical solution (VOZOFF, 1991), which leads to an inversion program that is fast and economical in terms of memory requirement.

When lateral variations exist in the geo-electrical structure, a full 2D or even 3D inversion may be required for better accuracy. In these cases, one can simply start with a homogeneous interpretive model and leave the iterations converge to a solution. The choice of a first guess that may already be an approximation of the true values sought in the inversion can reduce the processing time by requiring less iterations to converge.

In this paper, we apply a method to generate approximate first models for MT inversion, using 1D joint inversion of data from the whole set of sounding stations spread on a survey line. The method implements a 1D laterally constrained inversion (LCI) technique (MIORELLI, 2011) that is capable of performing inversion of large datasets, at a low computational cost. An analysis of the method is performed by applying it to synthetic data sets from two-dimensional models.

2 METHODOLOGY

1D inversion of data from a single MT sounding station can be performed to generate resistivity values for a sequence of homogeneous layers. This is an intrinsically ill-posed problem (HADAMARD, 1902), due to the limited amount of information in the data, the existence of several different sources of noise, and the complexity of the real geological structures, which is always greater than that of the interpretive model. Therefore, a stable solution will be achieved only with the inclusion of some kind of constraint on the parameters. Usually, smoothing constraints (CONSTABLE; PARKER; CONSTABLE, 1987) are used because they are simple to implement, and guarantee a solution, even if sometimes at the expense of a better fitting of the data.

Inverting each sounding separately can generate useful models. However, in most areas of interest there will be regions where the two-dimensional nature of the geo-electrical structures imposes itself on the observations, making it impossible to properly fit the sounding curves with synthetic data from layered models. In these cases, it is desirable that the inversion of one sounding be allowed to influence the inversion of its neighbouring soundings, in such way that the demand for fitting the data can be relaxed in favor of the demand to generate laterally smooth solutions.

The method described in this paper performs the joint inversion of data from a set of MT sounding stations, each one generating a sequence of resistivity values that represent a vertical column in a layered model. All columns, one for each measuring station have the same number of layers of the same thicknesses. The method applies lateral smoothing constraints (AUKEN; CHRISTIANSEN, 2004; AUKEN et al., 2005) between the resistivities in the same layers in the columns corresponding to adjacent sounding stations (Fig. 1).

In all the examples shown here the method is applied to synthetic data from 2D transverse magnetic (TM) propagation mode surveys. The observed data are the real $Re(\hat{Z}_1)$ and imaginary $Im(\hat{Z}_1)$ components of the apparent impedance vector. The interpretive model is a horizontal plane-parallel layered medium and the parameters are the logarithmic values of the resistivities of each layer (ZHDANOV, 2002; SANTOS, 2004).

Figure 1 – Example of the organization of parameters in a 2D structure. The red triangles represent sounding stations.

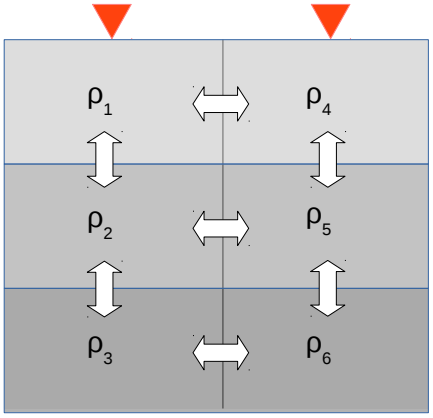

Source: From author

2.1 **Inversion theoretical revision**

Most of the geophysical problems are non-linear, meaning that the observed data are not a linear combination of the model parameters. A geophysical dataset **d**, with N_o observations, is to be fit by synthetic data generated from the N_p model parameters in vector **P**. The relationship between the synthetic data $\mathbf{d}_s$ and the parameter set is in the form

$$\mathbf{d}_s = \mathbf{F}(\mathbf{P}), \tag{2.1.1}$$

where **F** is an non-linear vector function that represents the forward modeling operator. This vector function also depends on the frequency ω, and on the measurement position (x, y, z).

Since the function **F** doesn't have a unique inverse, the problem of determining a set of parameters that generate synthetic data that approximate the observations is defined as that of minimizing a functional ϕ_d that measures the misfit of the model's forward response $\mathbf{F}(\mathbf{P})$ for a given set of parameters **P** to the observed data **d**:

$$\phi_d(\mathbf{P}) = \|\mathbf{d} - \mathbf{F}(\mathbf{P})\|^2 = [\mathbf{d} - \mathbf{F}(\mathbf{P})]^T [\mathbf{d} - \mathbf{F}(\mathbf{P})] \tag{2.1.2}$$

Optimization methods are used to find the solution of this type of problem, where the objective is to find the minimum of the data misfit functional ϕ_d, that is, to minimize the difference between observed data and calculated data. In this study, the minimization of the nonlinear functional ϕ_d, with respect to **P**, was performed iteratively by the Gauss-Newton method with the Marquardt's modification (MARQUARDT, 1963).

2.1.1 Regularized Inverse Problem

In geophysical applications, there is an infinite number of solutions that explain geophysical observations within experimental accuracy. One way of making this problem well-posed, is to introduce a priori information about the parameters to be estimated. This is done by including regularizing functionals ϕ_{REG} defined from a desired relationship between parameters, and acting not only as mathematical devices to stabilize the inverse geophysical problem, but also as constraints that reflect the geological and physical characteristics of the Earth's different environments.

After the introduction of regularization, the solutions to the inversion problem are obtained from the minimization of both ϕ_d and ϕ_{REG} as parts of a single function called objective function ϕ_α:

$$\phi_\alpha(\mathbf{P}) = \phi_d(\mathbf{P}) + \alpha\,\phi_{REG}(\mathbf{P}), \tag{2.1.3}$$

where α is a positive scalar, called the regularization parameter, which controls the relative weight of the information introduced by the regularizing functional to the inversion process.

In this work two regularization functions were used: Global Smoothness ϕ_{GS} and Total Variation ϕ_{TV}.

2.1.1.1 Global Smoothness

The Global Smoothness or first-order Tikhonov regularization (TIKHONOV; ARSENIN; JOHN, 1977) is the well-known Occam's inversion (CONSTABLE; PARKER; CONSTABLE, 1987) that leads to solutions in which the differences between parameter values are minimal, that is, variations between parameter values are smooth. The mathematical representation of the functional ϕ_{GS} is:

$$\phi_{GS}(\mathbf{P}) = \|\mathbf{SP}\|_2^2, \tag{2.1.4}$$

where $\mathbf{S}$ is a matrix which stores the relation between the parameters, each line being filled with 1 and -1 in the positions of the pairs of parameters to be related and zeros elsewhere.

The gradient vector $\mathbf{g}^{GS}$ and the Hessian matrix $\mathbf{H}^{GS}$ of ϕ_{GS} are, respectively:

$$\mathbf{g}^{GS} = \nabla_p \phi_{GS}(\mathbf{P}) = 2\mathbf{S}^t\mathbf{SP}, \tag{2.1.5}$$

$$\mathbf{H}^{GS} = \nabla_p \nabla_p^t \phi_{GS}(\mathbf{P}) = 2\mathbf{S}^t\mathbf{S}. \tag{2.1.6}$$

By minimizing the functional ϕ_α (Eq. 2.1.3) with the global smoothness

regularization, solutions are the parameters corresponding to the smoothest model that fits the data.

2.1.1.2 Total Variation

Smooth models representative of the subsurface geological structures are not always desirable. There are cases where sharp discontinuities in the resistivity, as in faults or intrusions, should be allowed in the models. The global smoothness regularization leads to solutions in which regions of discontinuities are detected, but softened in the solution model. On the other hand, the Total Variation regularizer does not penalize sharp variations, clearly marking the abrupt changes in the parameter values. The mathematical representation of the functional ϕ_{TV} is (MARTINS et al., 2011):

$$\phi_{TV}(P) = \sum_{i=1}^{N_d-1} |(P_{i+1} - P_i)|, \tag{2.1.7}$$

or in matrix form

$$\phi_{TV}(\mathbf{P}) = \|\mathbf{SP}\|_1. \tag{2.1.8}$$

However, if $P_{i+1} = P_i$, the functional ϕ_{TV} is not differentiable. To overcome this problem, (VOGEL, 1997) proposed the approximation:

$$\phi_{TV}(P) \cong \sum_{k=1}^{N_d} [(P_i - P_j)_k^2 + \beta]^{1/2}, \tag{2.1.9}$$

where β is a small and positive scalar.

The gradient vector and the Hessian of ϕ_{TV} are, respectively:

$$\mathbf{g}^{TV} = \mathbf{S}^T\mathbf{q}, \tag{2.1.10}$$

$$\mathbf{H}^{TV} = \mathbf{S}^T\mathbf{QS}, \tag{2.1.11}$$

where $\mathbf{q}$ is a vector given by

$$\mathbf{q} = \frac{(P_i - P_j)}{[(P_i - P_j)_k^2 + \beta]^{1/2}} \tag{2.1.12}$$

and $\mathbf{Q}$ is a diagonal matrix, with its non-zero values given by

$$\mathbf{Q} = \frac{\beta}{[(P_i - P_j)_k^2 + \beta]^{3/2}} \tag{2.1.13}$$

By minimizing the functional ϕ_α (Eq. 2.1.3) with the Total Variation regularization, solutions with abrupt variations between the parameters are preserved.

2.1.2 Gauss-Newton Method With Marquardt's Strategy

The objective function ϕ_α (Eq. 2.1.3) is treated as a second order approximation $\hat{\phi}_\alpha$ of ϕ_α around point $\mathbf{P}_k$, with the second order and higher derivatives equal to zero, since the non-linear geophysical functional is approximated by a linear function in $\mathbf{P}$.

$$\hat{\phi}_\alpha(\mathbf{P}) \simeq \phi_\alpha(\mathbf{P}_k) + \Delta\mathbf{P}_k^t \mathbf{g}_k^\alpha + \frac{1}{2}\Delta\mathbf{P}_k^t \mathbf{H}_k^\alpha \Delta\mathbf{P} \tag{2.1.14}$$

where $\Delta\mathbf{P}_k$ is the perturbation vector of the parameters, in the k-th iteration, and

$$\mathbf{g}_k^\alpha = (\nabla_\mathbf{P}\phi_\alpha)\mid_{\mathbf{P}=\mathbf{P}_k}, \tag{2.1.15}$$

$$\mathbf{H}_k^\alpha = (\nabla\nabla_\mathbf{P}^t\phi_\alpha)\mid_{\mathbf{P}=\mathbf{P}_k} \tag{2.1.16}$$

are, respectively, the gradient vector and the Hessian (second derivative matrix) of the functional ϕ_α, both with respect to the vector $\mathbf{P}$ evaluated in $\mathbf{P}_k$.

From the expansion of the functional ϕ_α in a Taylor series (Eq. 2.1.14) and taking into account that $\mathbf{g}_k^\alpha = \mathbf{g}_k^d + \alpha\,\mathbf{g}_k^{REG}$ and $\mathbf{H}_k^\alpha = \mathbf{H}_k^d + \alpha\,\mathbf{H}_k^{REG}$, we can rewrite Eq. 2.1.14 as:

$$\hat{\phi}_\alpha(\mathbf{P}) \simeq \phi_\alpha(\mathbf{P}_k) + \Delta\mathbf{P}_k^t(\mathbf{g}_k^d + \alpha\,\mathbf{g}_k^{REG}) + \frac{1}{2}\Delta\mathbf{P}_k^t(\mathbf{H}_k^d + \alpha\,\mathbf{H}_k^{REG})\Delta\mathbf{P}. \tag{2.1.17}$$

Then, the gradient vector of $\hat{\phi}_\alpha$ is calculated with respect to vector $\Delta\mathbf{P}_k$ and equated to the null vector, which results in (PUJOL, 2007):

$$(2\mathbf{A}^t\mathbf{A} + \alpha\,\mathbf{H}^{REG})\Delta\mathbf{P} = 2\mathbf{A}^t[\mathbf{d} - \mathbf{F}(\mathbf{P})] - \alpha\,\mathbf{g}^{REG}, \tag{2.1.18}$$

where $\mathbf{A}$ is the sensitivity matrix, defined as:

$$\mathbf{A}_{ij} = \frac{\partial\mathbf{F}_i(\mathbf{P})}{\partial\mathbf{P}_j}\mid_{\mathbf{P}=\mathbf{P}_k}. \tag{2.1.19}$$

Thus, in the k-th iteration, Eq. 2.1.18 is solved for $\Delta\mathbf{P}$ and the updated value of the parameter vector will be

$$\mathbf{P}_{k+1} = \mathbf{P}_k + \Delta\mathbf{P}_k \tag{2.1.20}$$

(MARQUARDT, 1963) suggests adding a factor λ (Marquardt coefficient) to the diagonal of the Hessian matrix to stabilize the steps of the process. It is a positive scalar and its value is changed during the inversion process, according to the analysis of the objective function $\hat{\phi}_\alpha$, in a given estimate, in relation to the previous estimate. If the objective function decreases ($\phi_\alpha(\mathbf{P}_{k+1}) < \phi_\alpha(\mathbf{P}_k)$), λ changes to $\frac{\lambda}{10}$. If the objective function increases ($\phi_\alpha(\mathbf{P}_{k+1}) > \phi_\alpha(\mathbf{P}_k)$), λ changes to 10λ. After the addition of the

Marquardt parameter, Eq. 2.1.18 turns to:

$$(2\mathbf{A}^t\mathbf{A} + \alpha\mathbf{H}^{REG} + \lambda\mathbf{I})\Delta\mathbf{P} = 2\mathbf{A}^t(\mathbf{d} - \mathbf{F}(\mathbf{P})) - \alpha\mathbf{g}^{REG} \tag{2.1.21}$$

where **I** is the identity matrix and the updated value of the parameter vector will be given by Eq. 2.1.20.

At a given iteration, if the objective function is close to the minimum, λ is sufficiently small compared to the elements of the Hessian and the method is closest to the Gauss-Newton method (Eq. 2.1.18). On the other hand, in regions far from the minimum point, λ becomes large compared to the elements of the Hessian, making the matrix $(2\mathbf{A}^t\mathbf{A} + \alpha\mathbf{H}^{REG} + \lambda\mathbf{I})$ diagonally dominant, and the iteration simply takes a small step in the downward direction of the gradient of $\hat{\phi}_\alpha$ (as in the Steepest Descent method).

3 APPLICATION

To illustrate the use of the inversion algorithm, we present its application to two different sets of synthetic data, generated by a 2D forward modelling finite element program, each one representing a specific geological structure. The synthetic data of each problem were contaminated with 2% Gaussian noise. The starting models for the examples presented here were a 200 Ohm-m homogeneous earth. The stability of the solution was tested by performing the inversion of the same data set contaminated with different random noise sequences.

3.1 **Model 1**

The first model (Fig. 2) represents a two-layer earth with a vertical fault. The data comprises ten equally spaced measuring stations, going from -5km to 5km, with 21 logarithmically spaced frequencies in the range of 0.1 Hz to 1000 Hz. Figure 3 shows the corresponding apparent resistivity and phase pseudo sections for model 1.

Figure 2 – Section view of model 1.

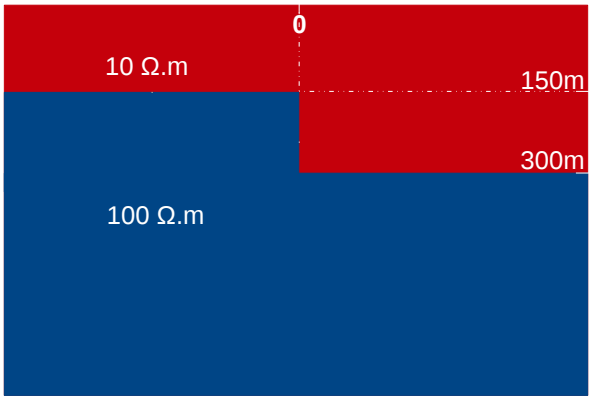

Source: From author

Figure 3 – TM mode apparent resistivity and phase pseudo sections.

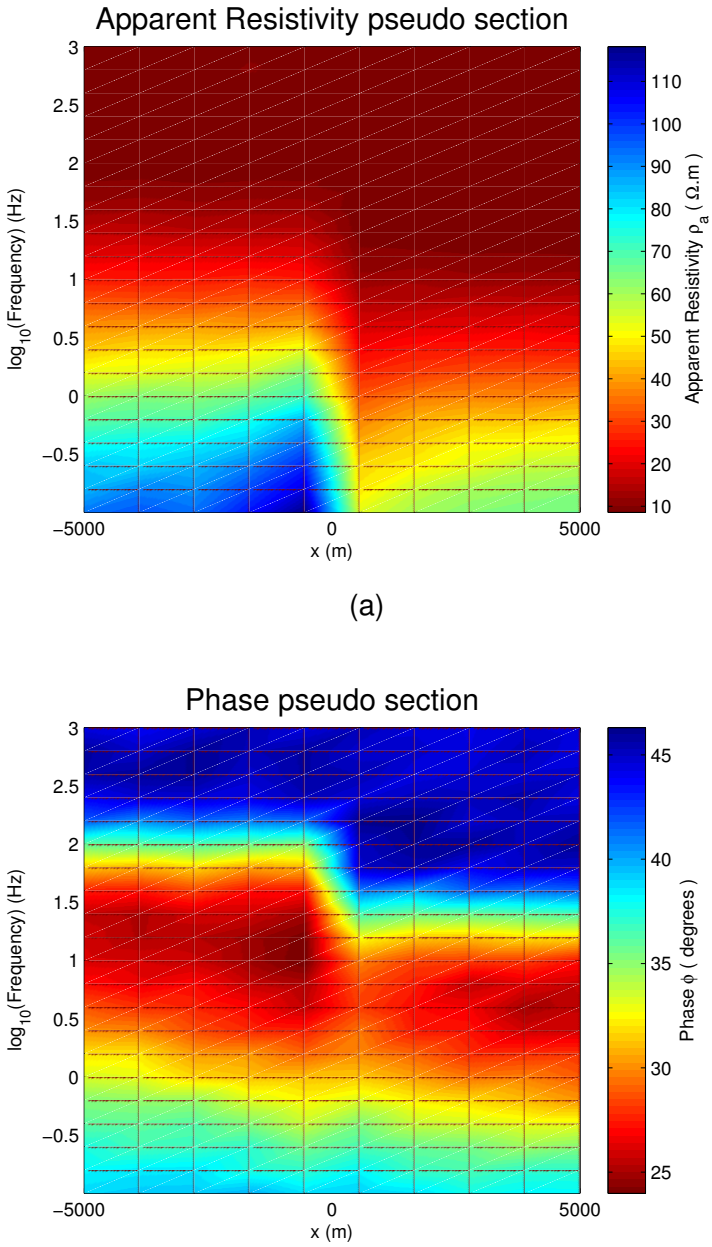

Source: From author

Except for the position of the fault, this model represents a layered earth, with a 150 m thick layer to the left of the fault and a 300 m thick layer to the right. Therefore, most sounding stations record data that can be well fit by a 1D interpretive model. Each sounding was inverted independently, as a usual 1D inversion, using the GS and TV constraints in the vertical direction only (Figs. 4a and 4b).

Figure 4 – Resistivity models obtained by 1D inversion using (a) Global Smoothness and (b) Total Variation regularization in the vertical direction and no lateral constraints.

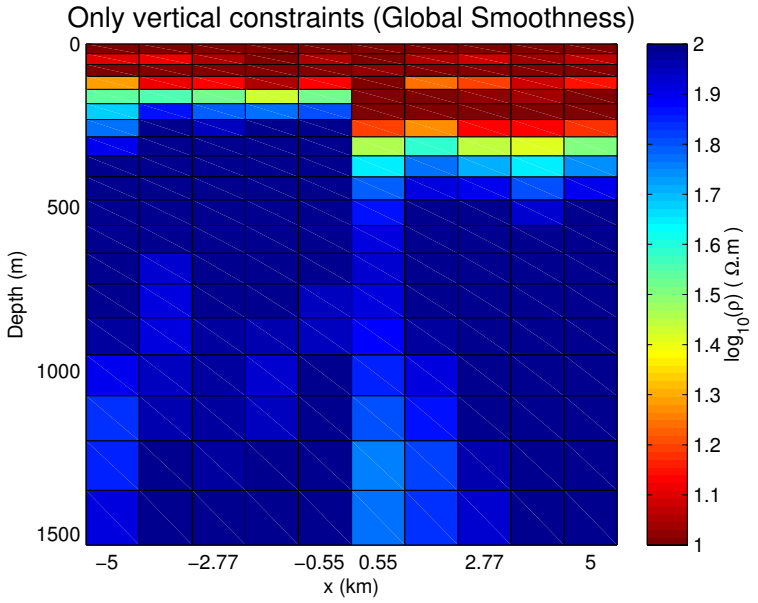

(a)

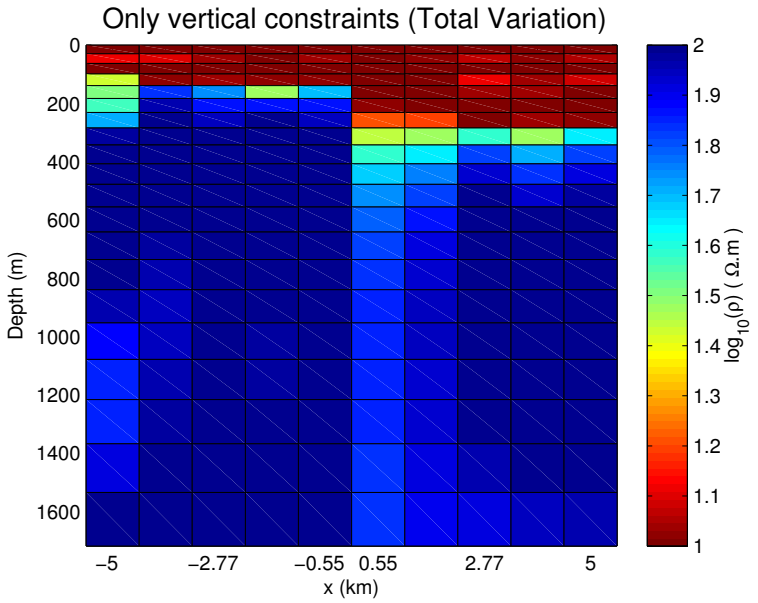

(b)

Source: From author

The independent 1D inversion of each sounding yields an approximation of the original model geometry. It can be noted that there is no big difference between the results using the GS and VT regularizations, except for the more oscillatory nature of the GS solution, which in this case is observed in the variations of the resistivities in each column. The resistivities of each layer are estimated to a good approximation

throughout the grid, except in the columns closest to the position of the fault where the vertical constraint creates an unwanted smoothing, creating a smudged area. Despite this, the fault itself is clearly resolved.

Because the model is predominantly 1D, that is, with no big lateral variations of resistivity, the independent 1D inversion of each sounding is good enough to determine the layer interfaces and its resistivities.

The estimated models obtained with the laterally constrained inversion (LCI) process using the GS and the TV regularizations are presented in Figures 5a and 5b, respectively.

Figure 5 – Resistivity models obtained by 1D LCI using (a) GS ($\lambda = 10^4$, $\alpha_V = 5 \times 10^{-7}$ and $\alpha_H = 5 \times 10^{-6}$) and (b) TV ($\lambda = 10^4$, $\alpha_V = 10^{-5}$, $\alpha_H = 10^{-4}$ and $\beta = 10^{-3}$) regularizations in both vertical and lateral directions.

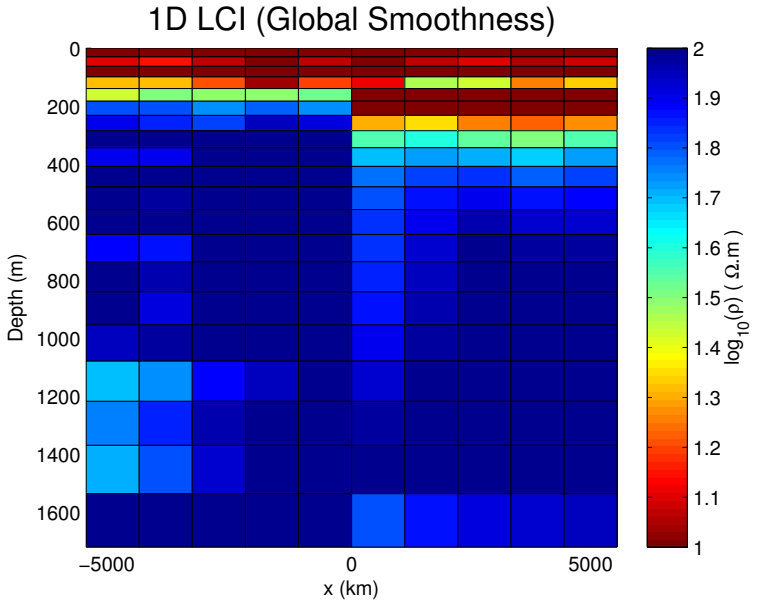

(a)

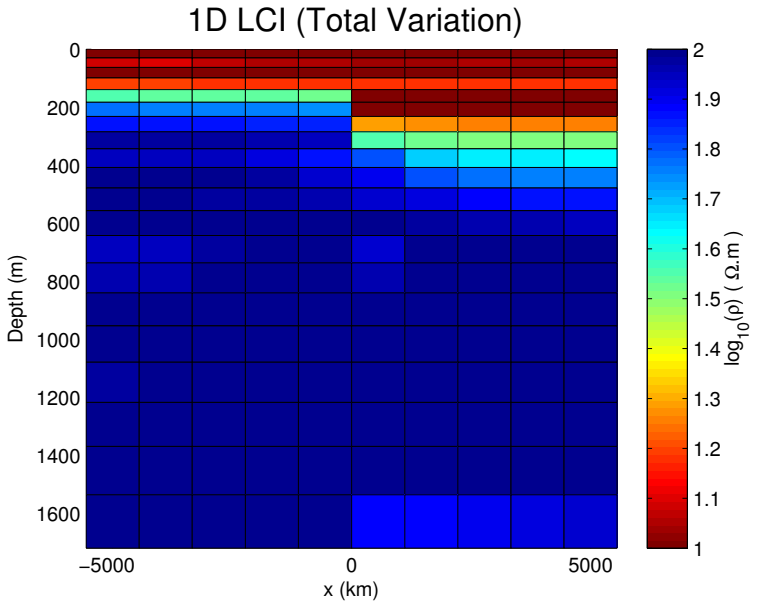

(b)

Source: From author

While Figure 5b is showing that the smudged area is decreased in the LCI result, being greater in the no lateral constraints result (Fig. 4b), Figs. 4a and 5a show that there is no big improvement caused by the lateral constraint.

An overall comparison of the results with and without the lateral constraint, for

the fault model, shows that the results are relatively close because the model is mostly constituted by laterally continuous structures, except for the fault.

So this case illustrates a situation in which it is better not to use lateral, specially smoothing, constraints because the lateral constraint improves little (or even does not improve) the final inversion result.

Figure 6 – Data fitting curves for the 1D LCI using GS: positions (a) $x = -5$km, (b) $x \simeq -0.55$km and (c) $x = 5$km.

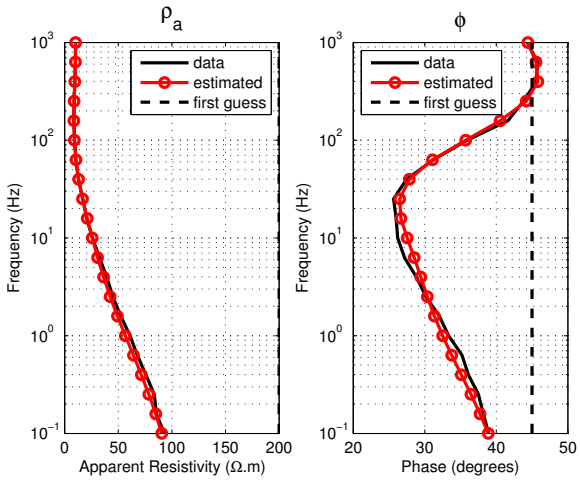

(a)

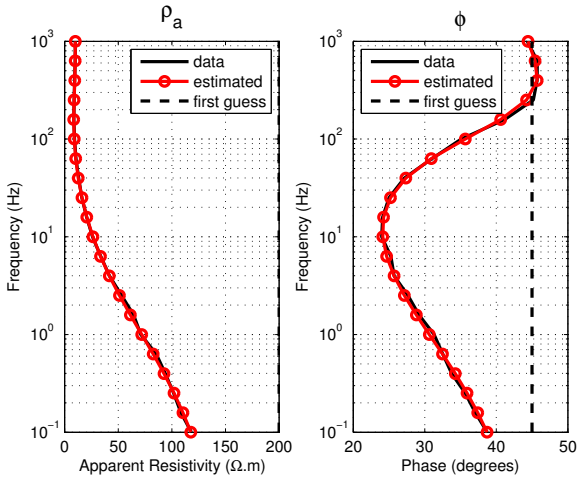

(b)

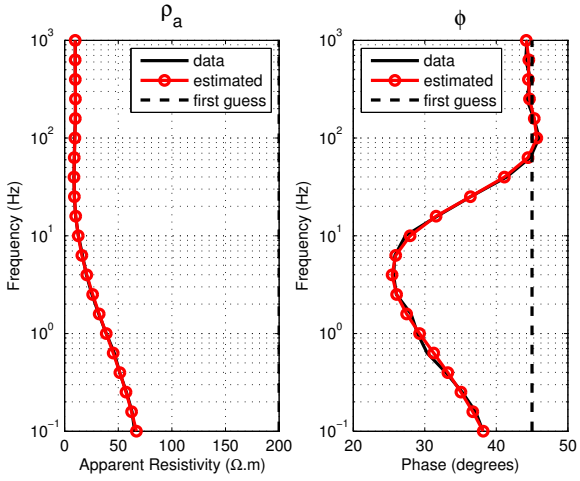

(c)

Source: From author

Figure 7 – Data fitting curves for the 1D LCI using TV: positions (a) $x = -5$km, (b) $x \simeq -0.55$km and (c) $x = 5$km.

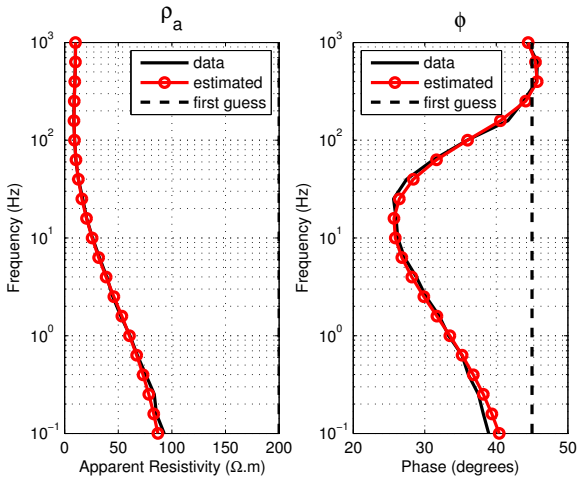

(a)

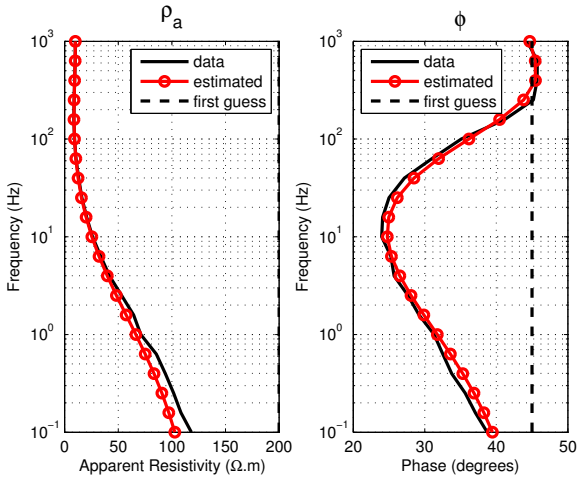

(b)

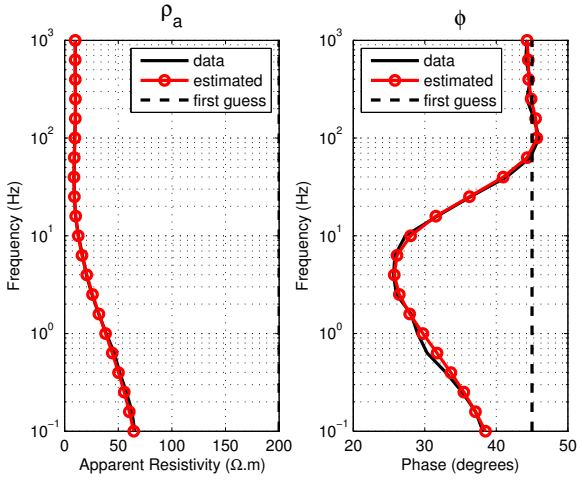

(c)

Source: From author

Figures 6b, 6c, 7b, and 7c show the data fitting for different sounding positions with the GS and TV regularizations, respectively. The whole data was well adjusted in both cases because there is no big lateral variations of resistivity.

3.2 **Model 2**

Figures 8 and 9 show the second model tested in this study and its corresponding apparent resistivity and phase pseudo sections. This is a two-layer model containing two conductive bodies (10 ohm.m) located in the upper layer. The data comprises 15 equally spaced measuring stations, going from -1km to 1km, with 21 logarithmically spaced frequencies, varying from 0.1Hz to 1000Hz.

Figure 8 – Section view of the model 2.

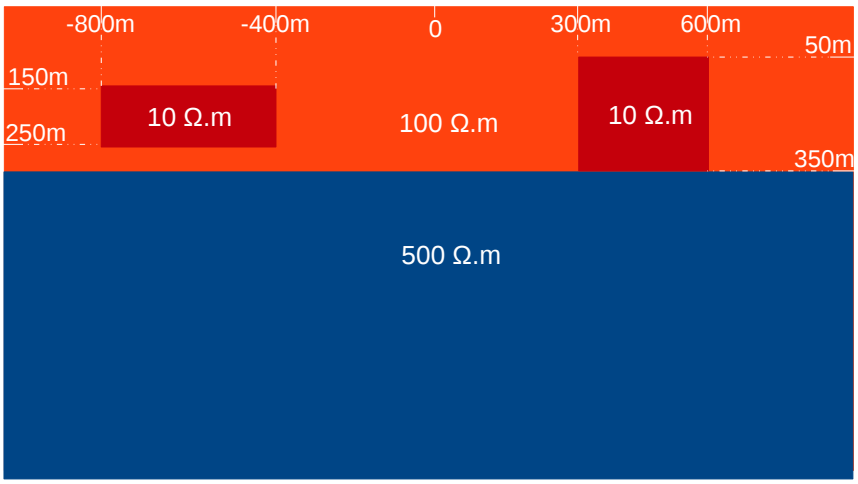

Source: From author

Figure 9 – TM mode apparent resistivity and phase pseudo sections.

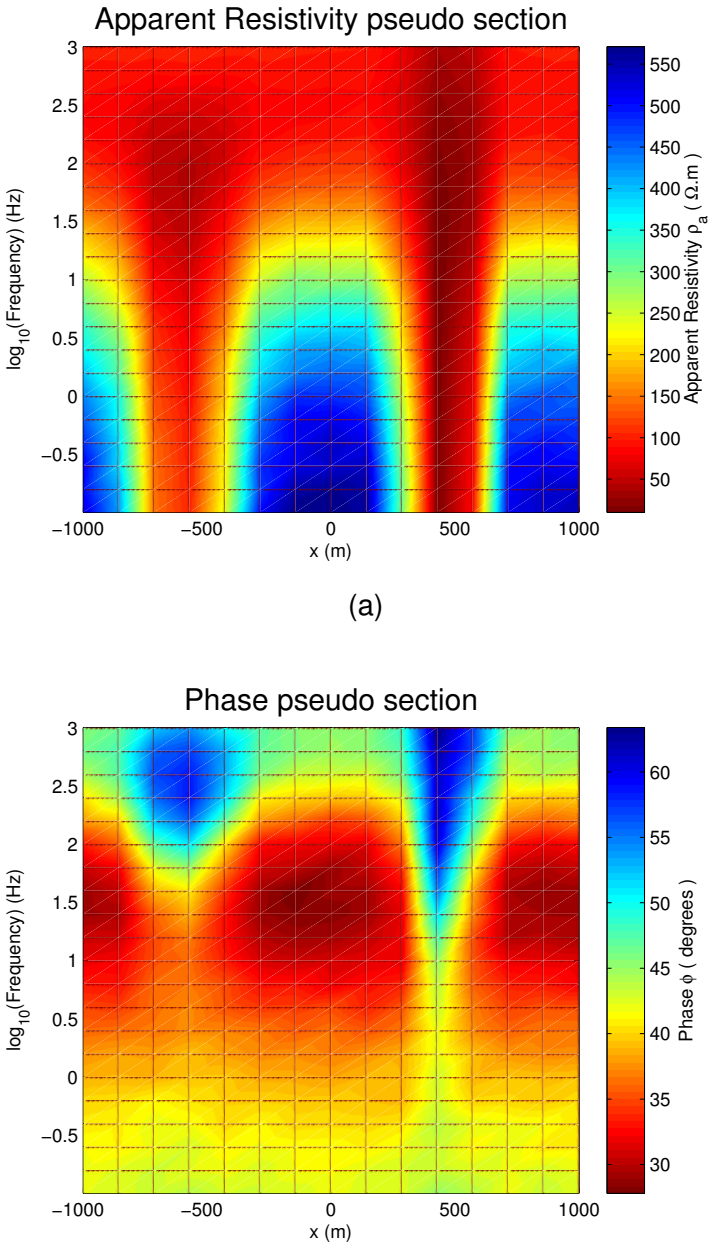

Source: From author

The inversion results using the GS and TV regularizations in the vertical direction only (no lateral constraints), are presented in Figures 10a and 10b, respectively.

Figure 10 – Resistivity models obtained by 1D inversion using (a) GS and (b) TV regularizations in the vertical direction and no lateral constraints.

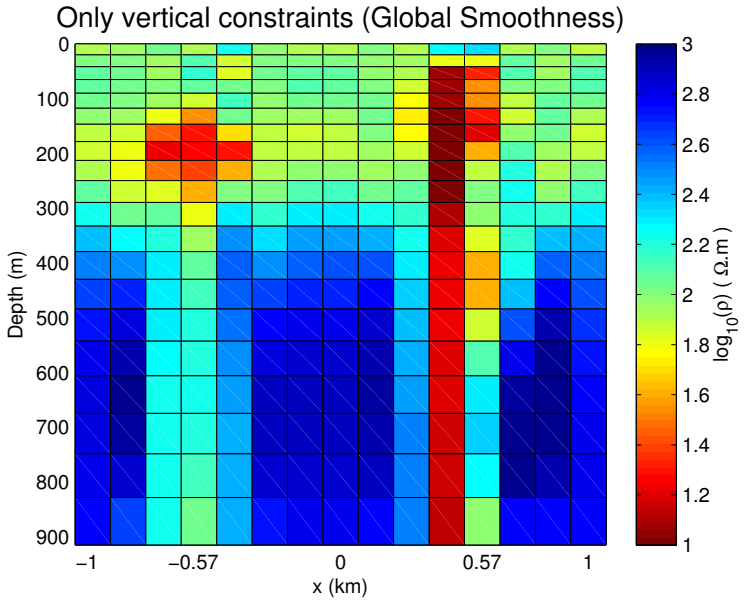

(a)

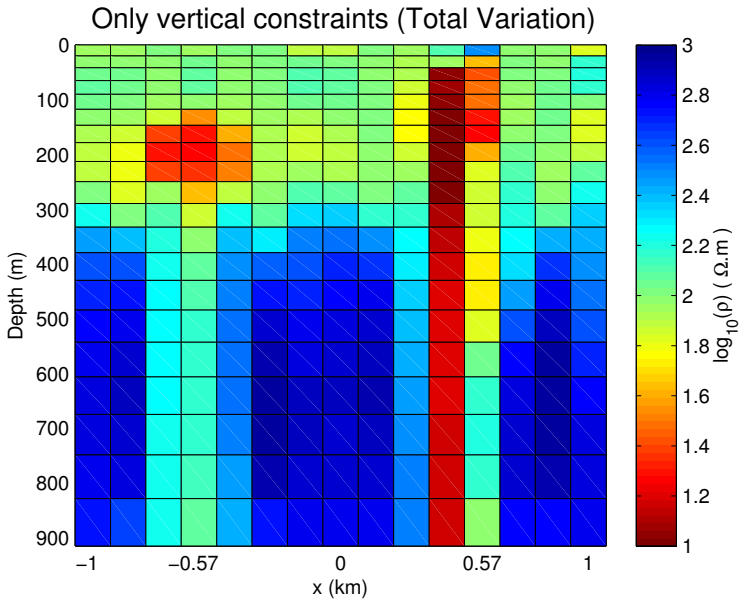

(b)

Source: From author

The vertical constraint creates an unwanted smoothing, with a smudged area below the location of each block. This shaded area is even bigger below the second block, probably because its base coincides with the horizontal interface. For this case, the independent 1D inversion of each sounding can not give a good solution, because now there's no station which isn't under the influence of the 2D structures.

The laterally constrained inversion (LCI) of the synthetic data generated by model 2 resulted in the resistivity models shown in the Figures 11a and 11b.

Figure 11 – Resistivity models obtained by 1D LCI using (a) GS ($\lambda = 10^4$, $\alpha_V = 10^{-5}$ and $\alpha_H = 3 \times 10^{-4}$) and (b) TV ($\lambda = 10^4$, $\alpha_V = 10^{-4}$, $\alpha_H = 5 \times 10^{-4}$ and $\beta = 10^{-2}$) regularizations in both vertical and lateral directions.

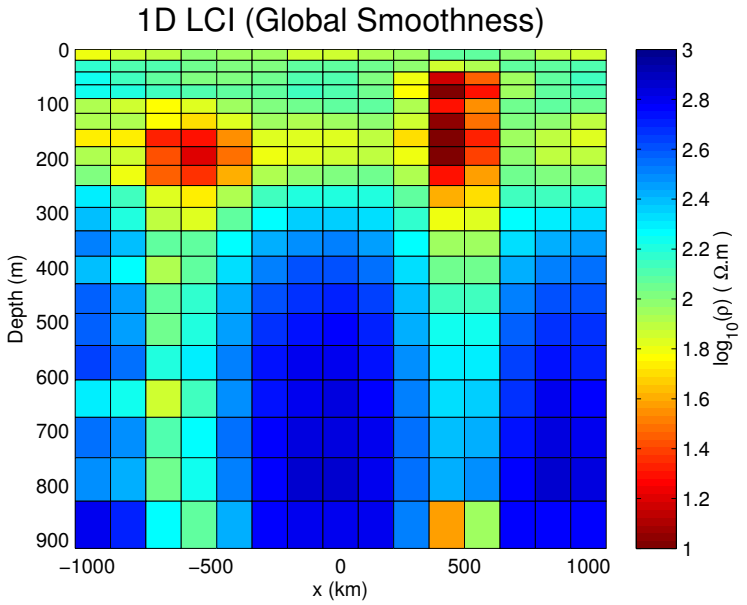

(a)

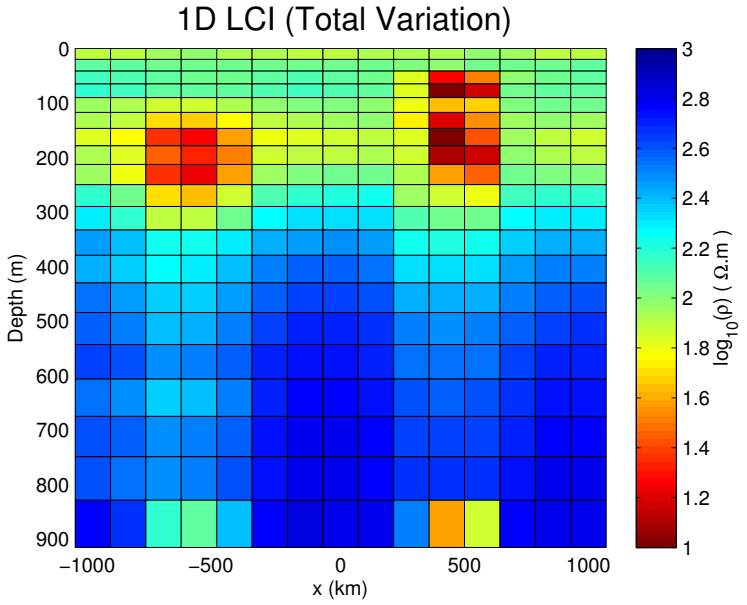

(b)

Source: From author

Both Figures 11a and 11b show good results in the sense of detecting the presence of the two conductive bodies and the position of the interface between the

layers. The effect of the vertical constraint, that spread the influence of the conductive bodies down through the columns, is now balanced by the influence of the lateral constraints, so the bodies are better delineated using the LCI.

The inversion result using the GS regularization is somewhat “over smoothned”. This is most noticeable is the positions below the conductive blocks, where the artifacts created by the vertical constraints are stronger. Because of that, the definition of the interface is impaired.

The inversion with the TV constraints (Fig. 11b) was more efficient in delineating the bodies both horizontally and vertically, despite the permanence of the vertical constraint effect.

Figure 12 – Data fitting curves for the 1D LCI using GS: positions (a) $x \simeq -0.57$km above the first block (b) $x = 0$km right in the middle of the two blocks and (c) $x \simeq 0.57$km above the second block.

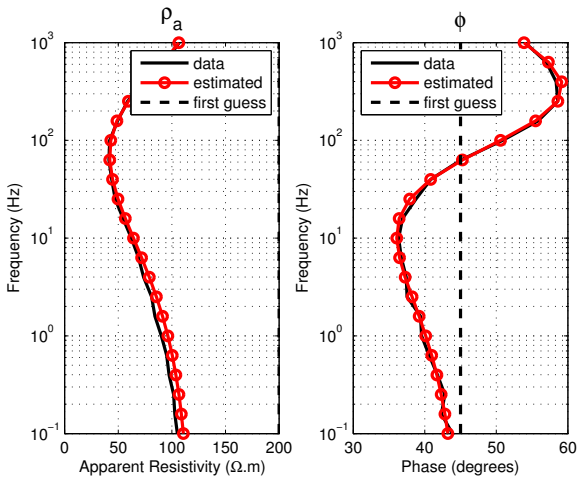

(a)

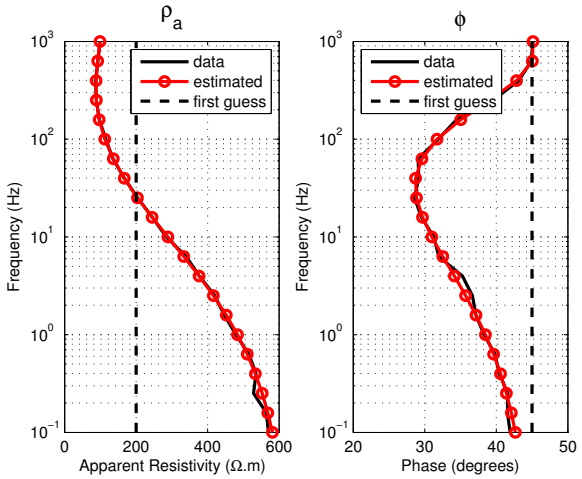

(b)

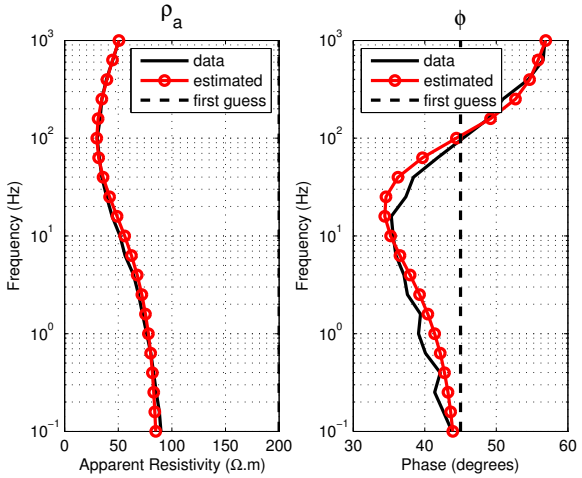

(c)

Source: From author

Figure 13 – Data fitting curves for the 1D LCI using TV: positions (a) $x \simeq -0.57$km above the first block (b) $x = 0$km right in the middle of the two blocks and (c) $x \simeq 0.57$km above the second block.

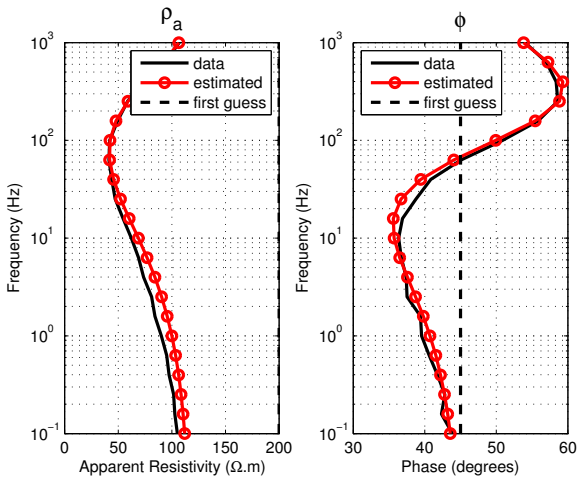

(a)

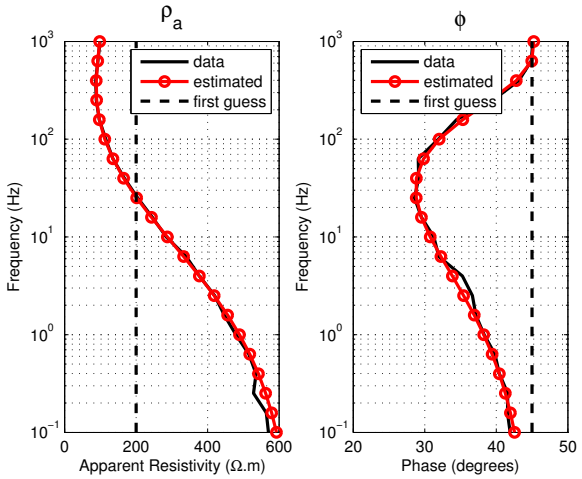

(b)

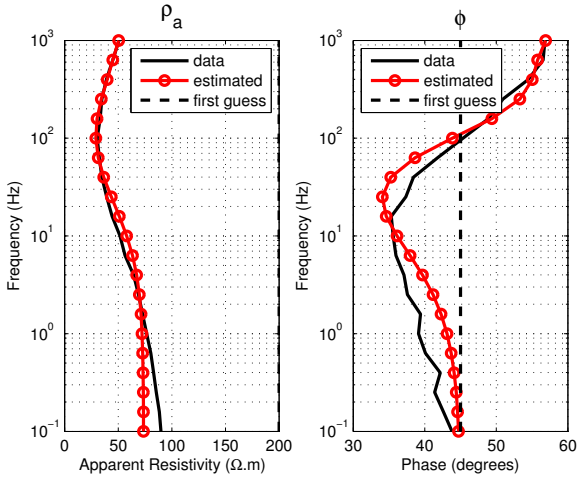

(c)

Source: From author

The apparent resistivity and phase curves are used to show the data fitting in Figures 12 and 13, with the GS and TV regularizations, respectively. Note that in this case the data can not be as well fit as in the first case (model 1), because now there's really no measuring station on a position far from the 2D structures.

4 CONCLUSION

The results show that the 1D laterally constrained inversion method applied to MT data is an effective way for delineating 2D geoelectrical structures. It generates very fast results in detecting 2D isolated structures, resulting in an efficient and inexpensive tool for quick imaging, especially on areas which can not be well approximated by layered models.

The Global Smoothness and Total Variation methods are sufficient to achieve the model solution. Moreover, the TV constraint improves the results at the edges of the body since it allows abrupt variations in the parameters.

For cases like the first model, where most of the geoelectrical structure is predominantly 1D, the LCI yields to no big improvements if compared to the results of the independent 1D inversion of each sounding. On the other hand, for cases like the second model, the LCI balances the effect of the vertical constraint and better delineates the conductive bodies.

The LCI results can be used as interpretive (initial) models of a 2D inversion algorithm, avoiding solutions that correspond to local minima.

REFERENCES

AUKEN, E.; CHRISTIANSEN, A. V. Layered and laterally constrained 2d inversion of resistivity data. **Geophysics**, SEG, v. 69, n. 3, p. 752–761, 2004.

AUKEN, E. et al. Piecewise 1d laterally constrained inversion of resistivity data. **Geophysical Prospecting**, EAGE, v. 53, n. 4, p. 497–506, 2005.

CONSTABLE, S. C.; PARKER, R. L.; CONSTABLE, C. G. Occam's inversion: a practical algorithm for generating smooth models from electromagnetic sounding data. **The Leading Edge**, SEG, v. 52, n. 3, p. 289–300, 1987.

HADAMARD, J. Sur les problèmes aux dérivées partielles et leur signification physique. **Princeton university bulletin**, v. 13, p. 49–52, 1902.

MARQUARDT, D. W. An algorithm for least-squares estimation of non-linear parameters. **J. of the Society for Industrial and Applied Mathematics**, v. 11, n. 2, p. 431–441, 1963.

MARTINS, C. M. et al. Total variation regularization for depth-to-basement estimate: Part 1 - mathematical details and applications. **Geophysics**, SEG, v. 76, n. 1, p. I1–I12, 2011.

MIORELLI, F. Joint laterally constrained inversion of csem and mt data. In: EAGE CONFERENCE & EXHIBITION INCORPORATING SPE EUROPEC, 73RD. **Extended Abstract**. Vienna, Austria, 2011.

PUJOL, J. The solution of nonlinear inverse problems and the Levenberg-Marquardt method. **Geophysics**, SEG, v. 72, n. 4, p. W1–W16, 2007.

SANTOS, F. A. M. 1d laterally constrained inversion of em34 profiling data. **Journal of Applied Geophysics**, Elsevier Science, v. 56, n. 2, p. 123–134, 2004.

TIKHONOV, A. N.; ARSENIN, V. Y.; JOHN, F. **Solutions of ill-posed problems**. [S.l.]: Winston Washington, DC, 1977.

VOGEL, C. R. Nonsmooth regularization. In: ENGL, H. W.; LOUIS, A. K.; RUNDELL, W. (EDS.). **Inverse problems in geophysical applications**. [S.l.]: Society for Industrial and Applied Mathematics, 1997. v. 88.

VOZOFF, K. 8. the magnetotelluric method. In: NABIGHIAN, M.N. (EDT.). **Electromagnetic methods in applied geophysics**: volume 2, application, parts a and b. [S.l.], 1991. p. 641–712.

ZHDANOV, M. S. **Geophysical inverse theory and regularization problems**. 1. ed. [S.l.]: Elsevier Science, 2002. (Methods in geochemistry and geophysics 36). ISBN 9780444510891,0444510893.